Lithuanian Journal of Physics
Vol. **64**, No. 3, pp. 189–202 (2024)
ISSN 1648-8504 eISSN 2424-3647
DOI: https://doi.org/10.3952/physics.2024.64.3.4

VARIATIONS OF BLACK CARBON, PARTICULATE MATTER AND NITROGEN OXIDES MASS CONCENTRATIONS IN URBAN ENVIRONMENT WITH RESPECT TO WINTER HEATING PERIOD AND METEOROLOGICAL CONDITIONS

D. Pashneva, A. Minderytė, L. Davulienė, V. Dudoitis, and S. Byčenkienė

SRI Center for Physical Sciences and Technology, Department of Environmental Research, Saulėtekio 3, 10257 Vilnius, Lithuania
Email: daria.pashneva@ftmc.lt

Received 12 March 2024; revised 3 June 2024; accepted 3 June 2024

The atmospheric concentrations of particulate pollution are of great scientific concern due to their impact on both human health and environment. This study aimed to investigate the concentration of black carbon (BC), particulate matter with an aerodynamic diameter of less than 10 micrometres (PM_{10}) and nitrogen oxides (NO_x) at an urban background environment throughout the year, and understand the impact of winter heating and meteorology on its concentration level. The campaign covered heating and non-heating periods, from 1 June 2021 to 31 May 2022. During the heating period, the mass concentrations of BC, PM_{10} and NO_x were 1.17, 24.9 and 19.4 μg m^{-3}, respectively. The analysis revealed that the mass concentrations of BC and NO_x were 1.9 and 1.4 times greater during the heating period, respectively, compared to the non-heating period. In contrast, PM_{10} remained almost constant during the heating (19.4 μg m^{-3}) and non-heating periods (20.0 μg m^{-3}). Throughout the year, the BC mass concentration was dominated by BC_{FF} (71.2%) originating from fossil fuel combustion with a maximum (8.43 μg m^{-3}) during the heating period. Moreover, wind speed presented a weak negative correlation with BC (r = –0.40), PM_{10} (r = –0.19) and NO_x (r = –0.40) during the heating period.

Keywords: air pollution, black carbon, source apportionment, fossil fuel, biomass burning

PACS: 92.60.Sz, 92.60.Mt, 92.60.hf

1. Introduction

Urban environments face complex challenges in maintaining air quality, particularly during the winter months when heating demand increases and meteorological conditions have a significant impact on pollution dispersion [1–4]. Among the variety of pollutants, aerosol particles PM_{10} containing black carbon (BC) stands out as an important contributor to human health risks [1] in urban environments. It can act as a carrier of other pollutants, including toxic compounds and heavy metals, contributing to the overall health risks associated with particulate pollution by infiltrating sensitive areas of the respiratory system and causing respiratory diseases, including asthma, chronic obstructive pulmonary disease and lung cancer [5–13]. Understanding the dynamics of BC mass concentration within urban settings, especially during the winter heating period, is important for effective air quality management and policy formulation [1, 2]. In remote environments, BC is a significant component of particulate aerosols and plays an important and distinctive role in the climate system by absorbing solar radiation, influencing the properties of clouds, and affecting snow and ice cover [10, 14].

Many European cities face air pollution challenges [15–17] with traffic being a significant contributor to BC emissions. BC levels show variability but are typically in the range of a few to several micrograms per cubic metre [2, 18, 19]. In urban areas, sources of BC are diverse, ranging from transport exhaust emissions to residential heating and industrial processes. However, the relative contributions of these sources can vary significantly depending on factors such as prevailing meteorological conditions and time of day [2, 3, 15, 18, 20]. This variability is particularly pronounced during periods of heavy traffic or adverse weather conditions, as has been extensively documented [21–23]. All these studies describe two daily peaks associated with morning and evening traffic, highlighting the difference between weekdays and weekends, as well as the difference between winter and summer concentrations. For instance, in Athens, the concentration of BC is higher during cold weather (2.4 μg m^{-3}) compared to warm weather (1.6 μg m^{-3}). There is a pronounced morning peak from 8 to 10 am and an evening peak at night. Additionally, the difference between weekdays and weekends is more noticeable during cold weather due to a lower traffic intensity during the weekend [22].

Generally, in Northern Europe BC mass concentration tends to be lower in comparison with Southern countries. The study carried out in Helsinki, Finland, reported BC_{FF} (BC from fossil fuel combustion) and BC_{BB} (BC from biomass burning) mass concentrations of 1.57 and 0.14 μg m^{-3}, respectively [18]. Conversely, research conducted in Zabrze, Poland, revealed higher BC mass concentrations, with BC_{FF} and BC_{BB} mass concentrations measured at 2.33 and 0.93 μg m^{-3}, respectively [2]. The results of the BC data analysis in Lithuania were published in several papers, covering different time periods and environments, i.e. covering the two-year period 2008–2009 [24], one year period of 2013 [25], the year and a half period from May 2013 to October 2014 [26]. Several scientific articles have analyzed the impact of extreme events, such as wildfires or volcano eruptions, on the Preila measurement site [27, 28]. Long-term BC variation in a background coastal site in Preila from 2008 to 2015 showed that the mean mass concentration of BC was 0.75 μg m^{-3}, with the highest values of 1.17 μg m^{-3} occurring in winter and gradually declining to a minimum concentration of 0.38 μg m^{-3} in summer. Studies conducted in urban environments have shown that the mass concentration of BC in Vilnius, Lithuania, was 0.77 μg m^{-3} during the warm period of May–August 2022 [29]. However, there is a dearth of studies on BC and meteorological factors in Lithuania.

Source apportionment studies employ different techniques such as chemical analysis, receptor modelling and dispersion modelling to distinguish between different emission sources and estimate their contributions to BC mass concentration [23, 30, 31]. Source apportionment for BC mass concentration measured by Aethalometer usually employs the Aethalometer Model proposed by Sandradewi et al., 2008 [32]. It was demonstrated that fossil fuel-related BC_{FF} from transport emissions constituted the majority of the total BC mass concentration, with an estimated range of 60–62%. In contrast, the biomass burning-related BC_{BB} input from residential heating was found to account for a smaller proportion, with an estimated range of 24–24% [18].

In urban environments, BC often coexists with NO_x emissions and interacts with each other through complex chemical and physical processes [33, 34]. For instance, traffic-related emissions are major sources of both BC and NO_x in urban areas and NO_x can be used as a tracer [3]. This study undertakes a comparative analysis of BC with both PM_{10} and NO_x to reveal their characteristics and temporal patterns during heating and non-heating periods in urban background environments.

2. Methods

2.1. Site description

The BC mass concentration measurements campaign was carried out from 1 June 2021 to 31 May 2022, on the roof of the SRI Center for Physical Sciences and Technology (FTMC) in Vilnius (54.72° N and 25.32° E), Lithuania (Fig. 1). The sampling site is situated approximately 8 km northeast of the city centre and about 600 m from a busy urban road, representing a wider area of the background environment of Vilnius.

In Lithuania, the warmest month of the year is July (18.3°C) and the coldest one is January (–2.9°C). In July 2021, the average temperature in Lithuania was 22.1°C, which is a positive anomaly of 3.8°C, making it the hottest July since 1961. Detailed information is provided in Subsection 3.3. The study considered the heating period to extend from October to March, distinguished by lower ambient temperatures and the use of residential heating. The non-heating period extends from April to September.

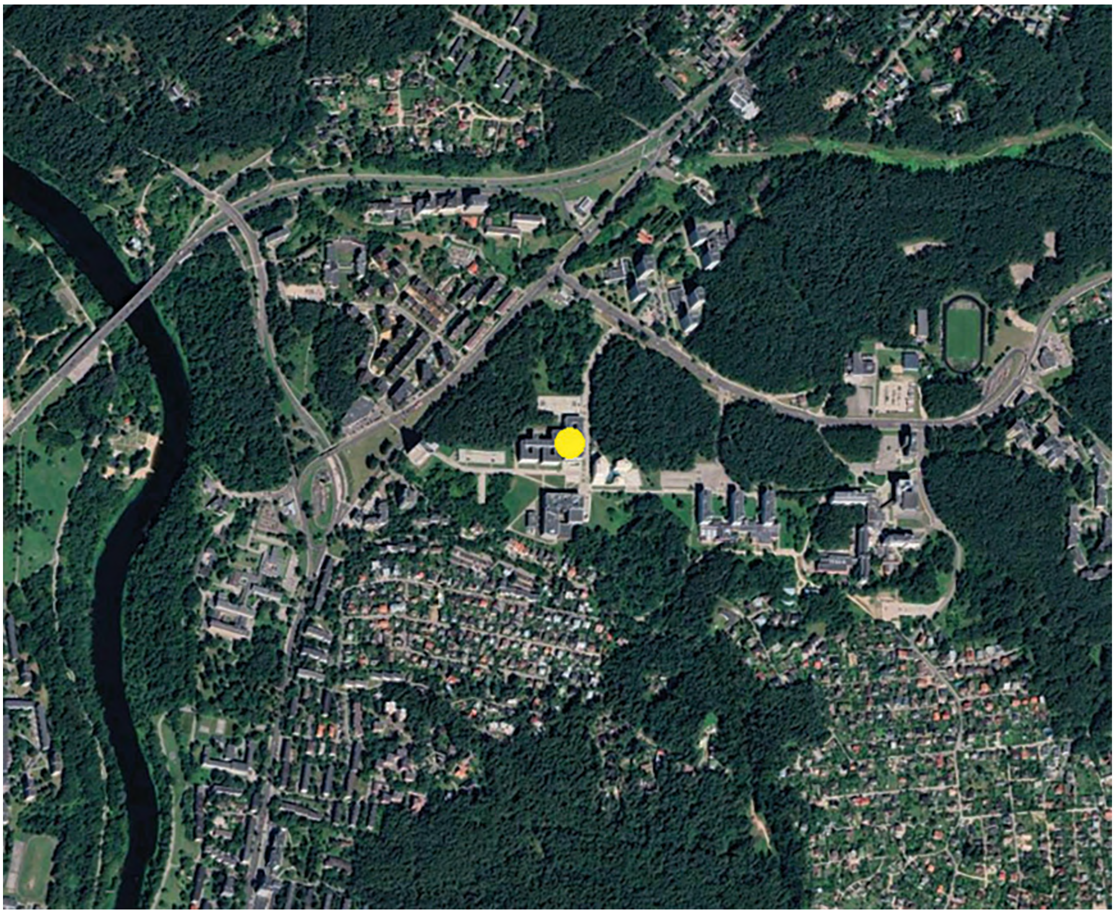

Fig. 1. Location of the sampling site (yellow dot) on the roof of SRI Center for Physical Sciences and Technology.

2.2. Black carbon mass concentration and source apportionment

Continuous real-time measurements of BC mass concentration were conducted using an Aethalometer Magee Scientific, model AE-31 (June–August 2021) and AE-33 (September 2021 – May 2022). The recorded data had a temporal resolution of 1 minute and a 4.9 L min^{-1} flow rate. The optical transmission of carbonaceous aerosol particles was measured sequentially at seven wavelengths (λ = 370, 470, 520, 590, 660, 880 and 950 nm). The standard channel for measuring BC is 880 nm. The aethalometer model proposed by Sandradewi et al., 2008 [32] was used to analyze the source apportionment data. This method uses the specific aerosol absorption Ångström exponent values for biomass burning (AAE_{BB}) of 2.2 and fossil fuels (AAE_{FF}) of 0.9. These values were determined for the background urban area in Vilnius, as discussed in the paper by Minderytė et al., 2022 [35]. This paper refers to the UTC+2 time zone. Hourly averages of BC mass concentrations were analyzed.

Hourly averages of temperature (°C), relative humidity (%), wind speed (m s^{-1}) and wind direction (degrees), along with the mass concentrations of air pollutants (NO_x and PM_{10}), were obtained from the Environmental Protection Agency of Lithuania (www.gamta.lt).

3. Results and discussion

3.1. Overview of the campaign

The descriptive statistics of the pollutants are given for the annual, non-heating and heating periods in Table 2. The annual mean BC mass concentration for the whole study period was 0.89 μg m^{-3} (standard deviation (SD) 0.99 μg m^{-3}) where the concentrations of BC_{BB} and BC_{FF} were 0.63 μg m^{-3} (SD 0.67 μg m^{-3})

Table 1. The descriptive statistics of the air pollution data during the heating, non-heating seasons and annual comparison ($\mu g\ m^{-3}$).

	BC	BC_{FF}	BC_{BB}	PM_{10}	NO_X
Heating season					
Mean	1.17	0.81	0.36	19.37	24.92
Median	0.23	0.59	0.22	16.48	16.63
Mode	0.26	0.23	0.03	10.0	14.34
SD	1.22	0.80	0.44	11.78	27.76
Min	0.04	0.03	0.01	0.07	4.40
Max	12.33	8.48	5.64	88.09	347.03
Non-heating season					
Mean	0.61	0.43	0.17	20.02	18.27
Median	0.43	0.29	0.12	17.77	13.00
Mode	0.16	0.05	0.01	14.0	9.56
SD	0.56	0.44	0.17	10.89	16.47
Min	0.01	0.01	0.01	1.00	3.44
Max	7.32	6.07	1.51	174.51	247.99
Annual					
Mean	0.89	0.63	0.27	19.68	21.62
Median	0.58	0.41	0.16	17.12	14.53
SD	0.99	0.67	0.35	11.36	23.10
Min	0.01	0.01	0.01	1.00	3.44
Max	12.33	8.48	5.64	174.51	347.03

and 0.27 $\mu g\ m^{-3}$ (0.35 $\mu g\ m^{-3}$), respectively, with a high SD indicating a high variability of concentrations during the analyzed period (Table 2). The highest seasonal differences in the non-heating and heating season averages (ratio in %) are observed for the BC mass concentration (63%) dominated by an increase of fossil fuel-originated BC_{FF} (72%) followed by the NO_x (31%) concentration. It should be noted that the median of BC level decreased (–61%) during the heating period, meaning that mass concentrations have an asymmetrical distribution.

It was found that pollutant concentrations had a clear monthly variation, being highest for all species (BC, including BC_{BB} and BC_{FF}, PM_{10} and NO_x) in March (during the heating period), with average monthly concentrations of 1.96, 0.68, 1.28, 27.83 and 35.43 $\mu g\ m^{-3}$, respectively. The highest mass concentrations during the non-heating period were observed in May for BC (0.73 $\mu g\ m^{-3}$), BC_{FF} (0.58 $\mu g\ m^{-3}$), and in August for BC_{BB} (0.25 $\mu g\ m^{-3}$). The lowest mass concentrations were observed in September for BC (0.5 $\mu g\ m^{-3}$) and BC_{BB} (0.05 $\mu g\ m^{-3}$), and in July for BC_{FF} (0.31 $\mu g\ m^{-3}$).

The typical patterns of BC mass concentrations during heating and non-heating periods according to histograms indicated a lognormal distribution (Fig. 3, Table 1). The frequency distribution of

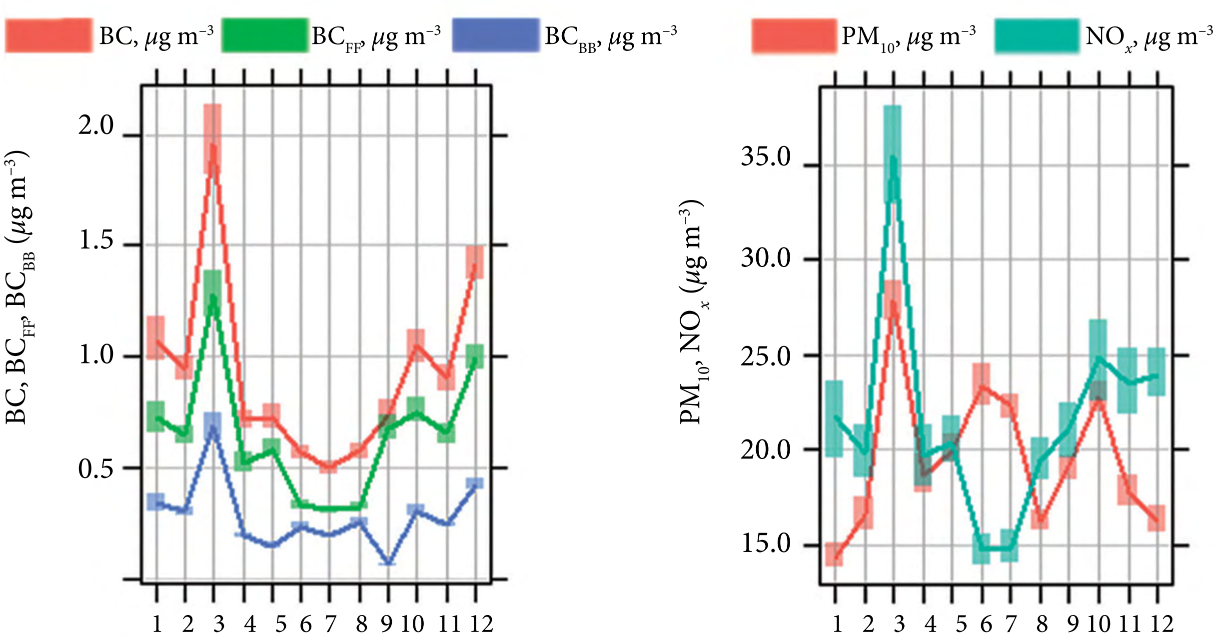

Fig. 2. Monthly means and 95% confidence intervals of BC, BC_{FF}, BC_{BB}, PM_{10} and NO_x mass concentrations during the year.

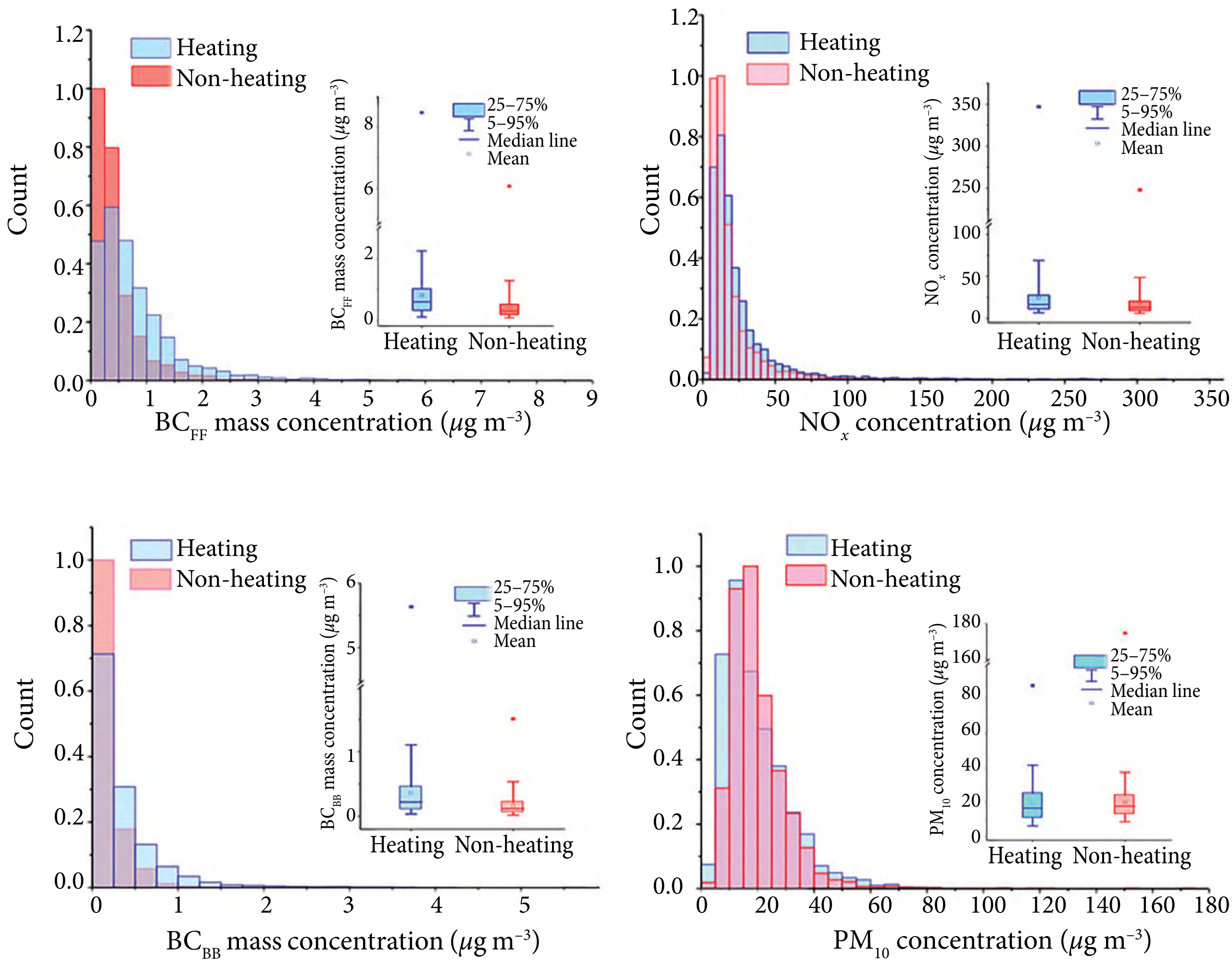

Fig. 3. Histogram showing the distribution of concentrations and box plots of the hourly mean BC_{FF}, BC_{BB}, NO_x and PM_{10} concentrations during heating and non-heating periods.

hourly concentrations was analyzed for the heating and non-heating periods with an interval of 0.25 μg m^{-3} for BC_{FF} and BC_{BB}, and 5.00 μg m^{-3} for PM_{10} and NO_x (Fig. 2).

The lowest concentrations of fossil fuel combustion originated BC_{FF} and biomass burning originated BC_{BB} dominated for the non-heating period in comparison to the heating period. The data suggests that there were more relatively clean days during the non-heating period, as also indicated by the significantly higher frequency of NO_x lower concentrations. However, the frequency of the heating period was significantly higher only for PM_{10} concentration in the range of up to 15.00 μg m^{-3}. As shown in Table 1, the PM_{10} concentration outliers in the heating period were below 90.00 μg m^{-3}. In comparison, the outliers in the non-heating period were concentrated below 175.00 μg m^{-3}.

During the study period, there were three days when the daily mean concentration of PM_{10} exceeded the EU air quality standard of 50.00 μg m^{-3} per 24 h and a permitted exceedance of 35 days per year. Two of these days occurred during the heating period and one day occurred during the non-heating period. It should be noted that there were no significant changes in the mean PM_{10} concentrations observed in Vilnius between the heating (19.37 μg m^{-3}) and non-heating (20.02 μg m^{-3}) period. In contrast, other cities showed a marked difference in concentrations between the two seasons. For example, in Italy, the concentration of PM_{10} increased by an average of 9.36 μg m^{-3} during the winter months, which was attributed to increased household heating [6, 3].

The obtained annual mean mass concentration of BC (0.89 μg m^{-3}) in Vilnius is comparable with those of many sites in Europe during different periods, for example, in Helsinki, Finland (1.69 μg m^{-3}, October 2015 – May 2017) [18], Madrid, Spain (2.33 μg m^{-3}, 2014–2015) [36], and Sofia, Bulgaria (3.6 μg m^{-3}, October 2020 – January 2021) [19]. For PM_{10}, the annual average concentration was found to be 19.68 μg m^{-3}, which is comparable to the ones obtained in Latium Region, Italy (21.90 μg m^{-3}, 2006–2012) [7], Ciuc Basin, Romanian Carpathians (19.00 μg m^{-3}, 2008–2016) [6] and Germany (18.10 μg m^{-3}, 2015–2018) [37].

3.2. Diurnal and weekly variations of BC mass concentrations

During the heating period, the concentrations of BC, BC_{FF}, BC_{BB} and NO_x were consistently higher throughout the week, as shown in Fig. 4, and exhibited higher concentrations on weekdays in comparison to weekends (Saturday and Sunday). The lower volume of traffic on weekends is likely the cause of this. Concentrations were slightly lower on Mondays, possibly due to reduced emissions from weekend traffic. PM_{10} concentrations, however, were lower from Wednesday to Saturday.

Figure 5 shows the average hourly fluctuations of BC_{FF}, BC_{BB}, NO_x and PM_{10} during both seasons. Although the pattern observed in both seasons is nearly the same, the hourly variation of BC, BC_{FF} and BC_{BB} averages is significantly higher in the heating season compared to that of the non-heating season. This can be attributed to variations in heating emissions and weather conditions.

During the heating period, the diurnal variation range of BC, BC_{FF} and BC_{BB} was large reaching up to 0.76, 0.52 and 0.27 μg m^{-3}, respectively. The diurnal variation of BC, BC_{FF} and BC_{BB} concentrations showed a typical urban pattern with a well-defined morning and evening emission

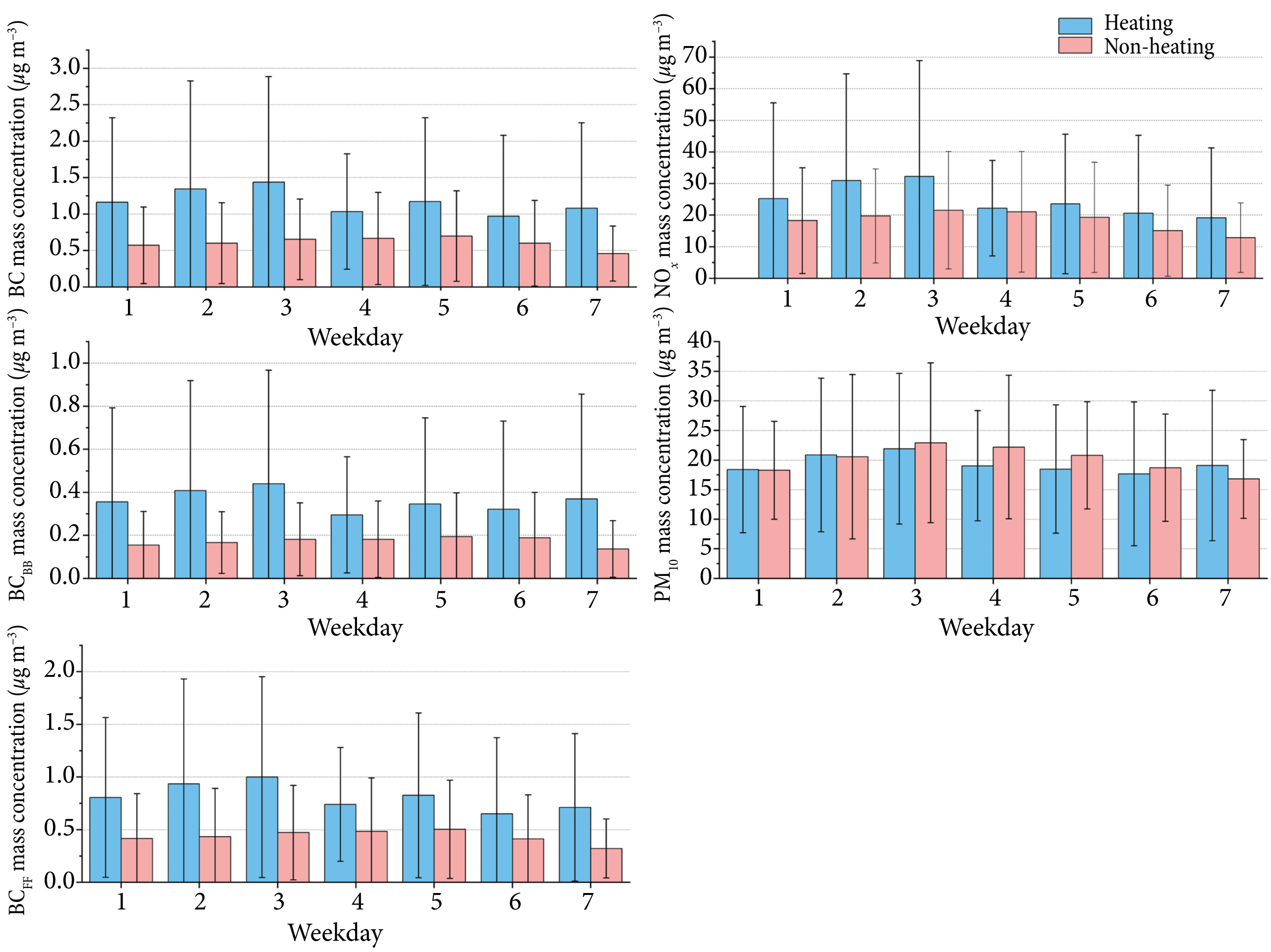

Fig. 4. Day-of-week mean concentrations of BC, BC_{FF}, BC_{BB}, PM_{10} and NO_x mass concentration at the heating and non-heating periods.

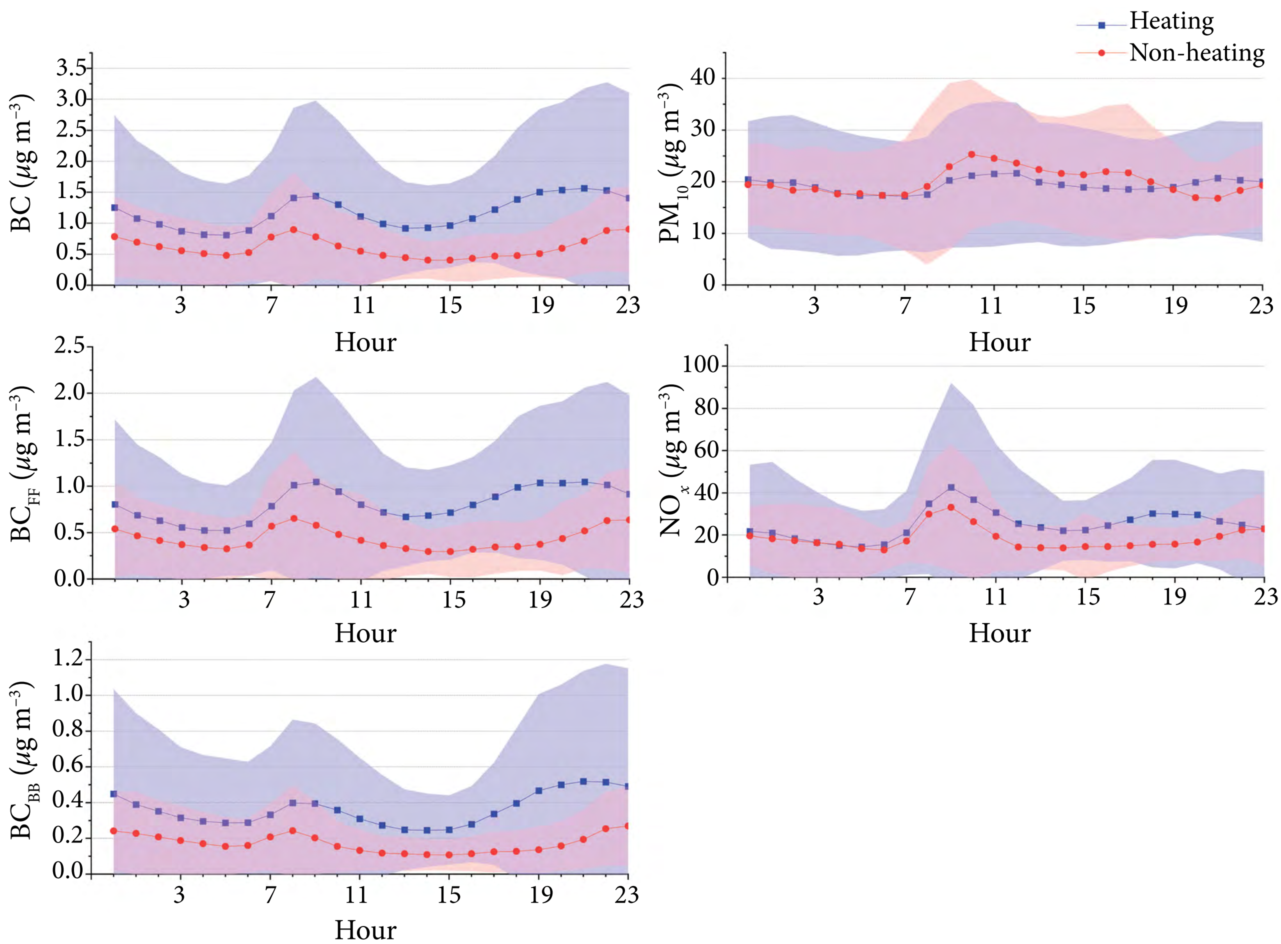

Fig. 5. Diurnal variation of hourly mean concentrations of BC, BC_{FF}, BC_{BB}, NO_x and PM_{10} during the heating and non-heating periods.

peak. The morning peak, which was primarily attributable to the morning rush hours, occurred between 7:00 and 9:00 for both periods. The peak concentrations during the heating period for BC, BC_{FF} and BC_{BB} were 1.44, 1.05 and 0.39 μg m^{-3}, respectively. During the non-heating period, the morning peak concentrations were 0.90, 0.65 and 0.24 μg m^{-3} for BC, BC_{FF} and BC_{BB}, respectively. The evening peak for the heating period was observed from 16:00 to 21:00. The main contributors to this peak could be attributed to evening rush hour and residential heating. The peak concentrations for BC, BC_{FF} and BC_{BB} were 1.57, 1.05 and 0.52 μg m^{-3}, respectively. For the non-heating period, the evening peak was observed from 19:00 to 23:00 (peak concentrations of 0.90, 0.64 and 0.27 μg m^{-3} for BC, BC_{FF} and BC_{BB}, respectively).

A similar diurnal variation in BC mass concentrations has been observed in European cities, e.g. in Galicia, Barcelona and Granada, Spain [20], and in Ostrava, Czech Republic [15]. Kucbel et al., 2017 [15] noted that these differences are likely to be related to the combination of anthropogenic emissions (from domestic heating and traffic), meteorology, and boundary layer dynamics, which favours the accumulation of pollutants.

The pattern of PM_{10} and NO_x observations during both seasons is almost identical between 00:00 and 16:00. However, it is notable that the concentrations are slightly higher during the heating period. Although the pattern of NO_x during both seasons is almost similar, the daily variation of mean concentrations of NO_x in the heating period is significantly higher compared to that of the non-heating period due to the variability of traffic emissions and prevailing meteorological conditions such as a lower mixing layer height [38]. The lowest concentrations of NO_x were observed during the early morning (from 01:00 to 06:00 for the heating period and from 00:00 to 07:00 for the non-heating period) and afternoon (from

12:00 to 19:00 for the non-heating period) due to a very low or no traffic at night-time and due pollutant dispersion during the daytime. Subsequently, there was an increasing tendency of NO_x from 07:00 to 11:00 for both seasons and from 17:00 to 21:00 for the heating period. The first peak can be due to the increasing morning traffic intensity, while the second peak due to the evening traffic rush hour.

3.3. Supporting meteorological evidences for BC source apportionment results

It is important to consider the influence of meteorological conditions on the pollution level during both heating and non-heating periods. The descriptive statistics for the meteorological variables during the heating and non-heating periods are presented in Table 2.

During the heating season, the mean temperature was 1.1°C, ranging from –15.6°C to 17.7°C. In contrast, during the non-heating period, the mean outdoor temperature was higher and reaching 14.8°C, with a range from –4.9 to 35.5°C. The average relative humidity level varied from 20 to 97%, with a mean of 81% and, similarly, from 18 to 97% with a mean value of 70% for heating and non-heating periods, respectively. During the heating period, the most common wind direction was WNW (19.5% of the total), followed by South (12.8%) and NW (10.5%). For the non-heating season, the dominant direction was associated with NW (17%), followed by WNW (12.9%), NE (9.0%) and ENE (8.5%). Figure 6 displays the correlation analysis of BC, BC_{FF}, BC_{BB}, NO_X and PM_{10} during the heating and non-heating periods.

A relatively strong positive correlation of BC ($r = 0.65$) with NO_x was observed during the heating period. Conversely, during the non-heating period, BC, BC_{FF}, BC_{BB} and PM_{10} concentrations exhibited a weak to moderate positive correlation with NO_x concentrations (Fig. 5). Furthermore, there has been a decrease in the absolute value of negative correlation between BC, BC_{FF}, BC_{BB}, NO_x, PM_{10} and wind speed (Fig. 6).

Although no correlations were observed between the BC mass concentration and the wind direction, visualizing mass concentration as a function of wind direction and speed using a polar plot can provide valuable insights into the spatial and temporal variability of air pollution providing a comprehensive understanding. Figure 6 shows the mean mass concentrations of BC, BC_{FF}, BC_{BB}, NO_x and PM_{10} as a function of wind speed and direction for each period, using a polar coordinate system. The colour scale indicates the average concentration levels and intervals of wind speed (ws, m s^{-1}). During the heating period, the polar plot for BC, BC_{FF}, BC_{BB}, NO_x and PM_{10} indicates that the sources (>2.0 μg m^{-3} for BC, >1.2 for BC_{FF}, >0.8 μg m^{-3} for BC_{BB}, 30.0 and 50.0 μg m^{-3} for PM_{10} and NO_x) are homogeneously distributed around the sampling site for all wind directions and wind speeds up to 0.5 m s^{-1}.

The polar plots during the non-heating period show the dominant influence of 2 sources. One is a local source around the site and the other is from a SW–SE direction. The highest concentrations of BC (above 0.70 μg m^{-3}) occur at the lowest wind speed during calm days, suggesting that there are local emissions distributed around the site and at wind speeds above 2.5 m s^{-1}. In contrast, the PM_{10} source during the non-heating period does not have a uniform distribution around the site and has an additional source from the NE with a higher wind speed 3–3.5 m s^{-1}. The observed patterns of seasonal variations in BC mass concentrations could be attributed to its characteristic as a fine aerosol with a longer residence time.

Table 2. The descriptive statistics of meteorological parameters during heating and non-heating periods.

	Heating period				Non-heating period			
	Min	Mean	Max	SD	Min	Mean	Max	SD
Temperature, °C	–15.6	1.1	17.7	5.6	–4.9	14.8	35.5	7.6
Relative humidity, %	20.0	81.0	97.0	17.0	18.0	70.0	97.0	20.0
Pressure, hPa	960.0	994.0	1026.0	13.0	962.0	994.0	1011.0	7.0
Wind speed, m s^{-1}	0.11	1.00	3.27	0.50	0.10	0.64	3.13	0.42

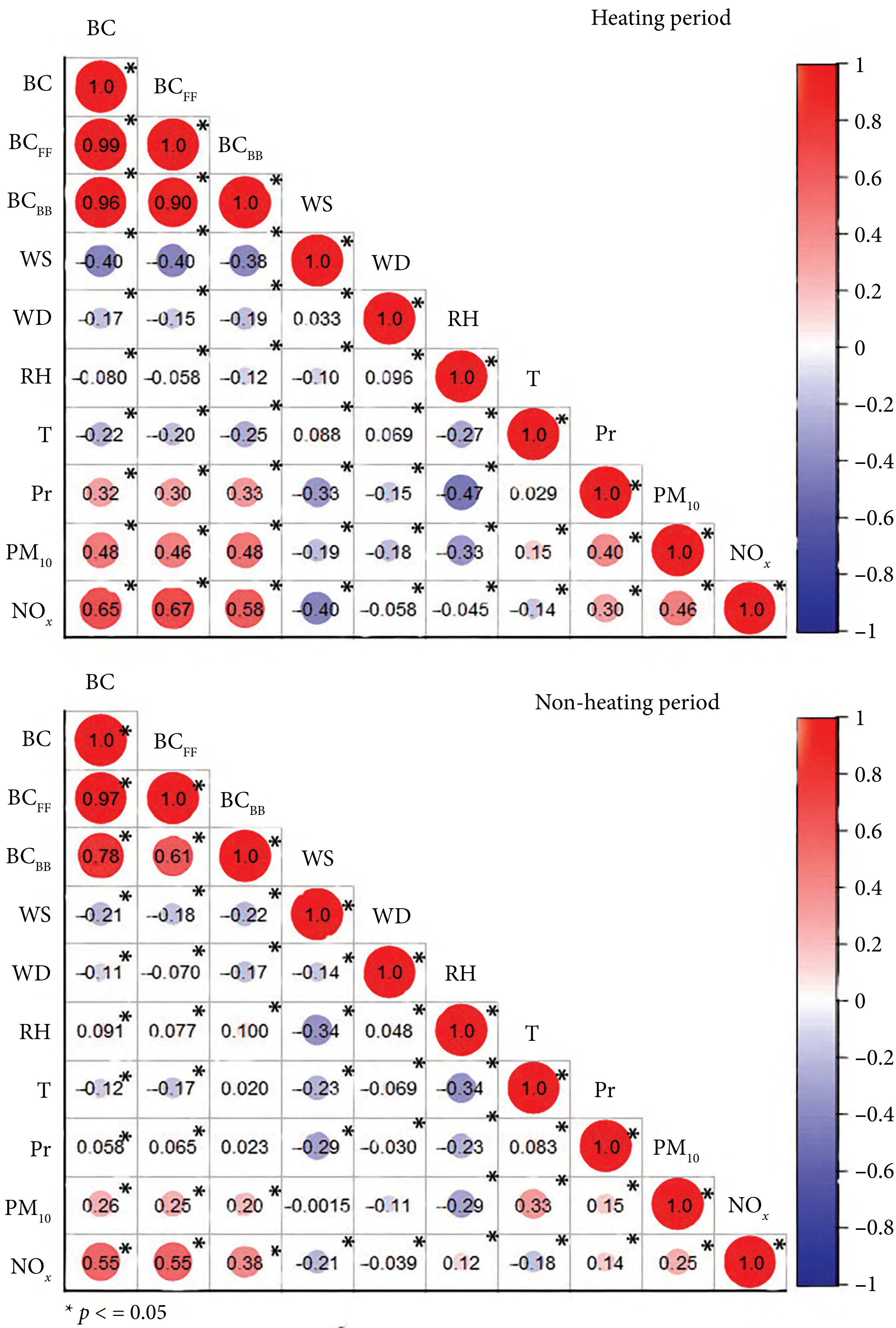

Fig. 6. Correlation analysis of BC, BC_{FF}, BC_{BB}, NO_x and PM_{10} during the heating and non-heating periods, * represents $p < = 0.05$.

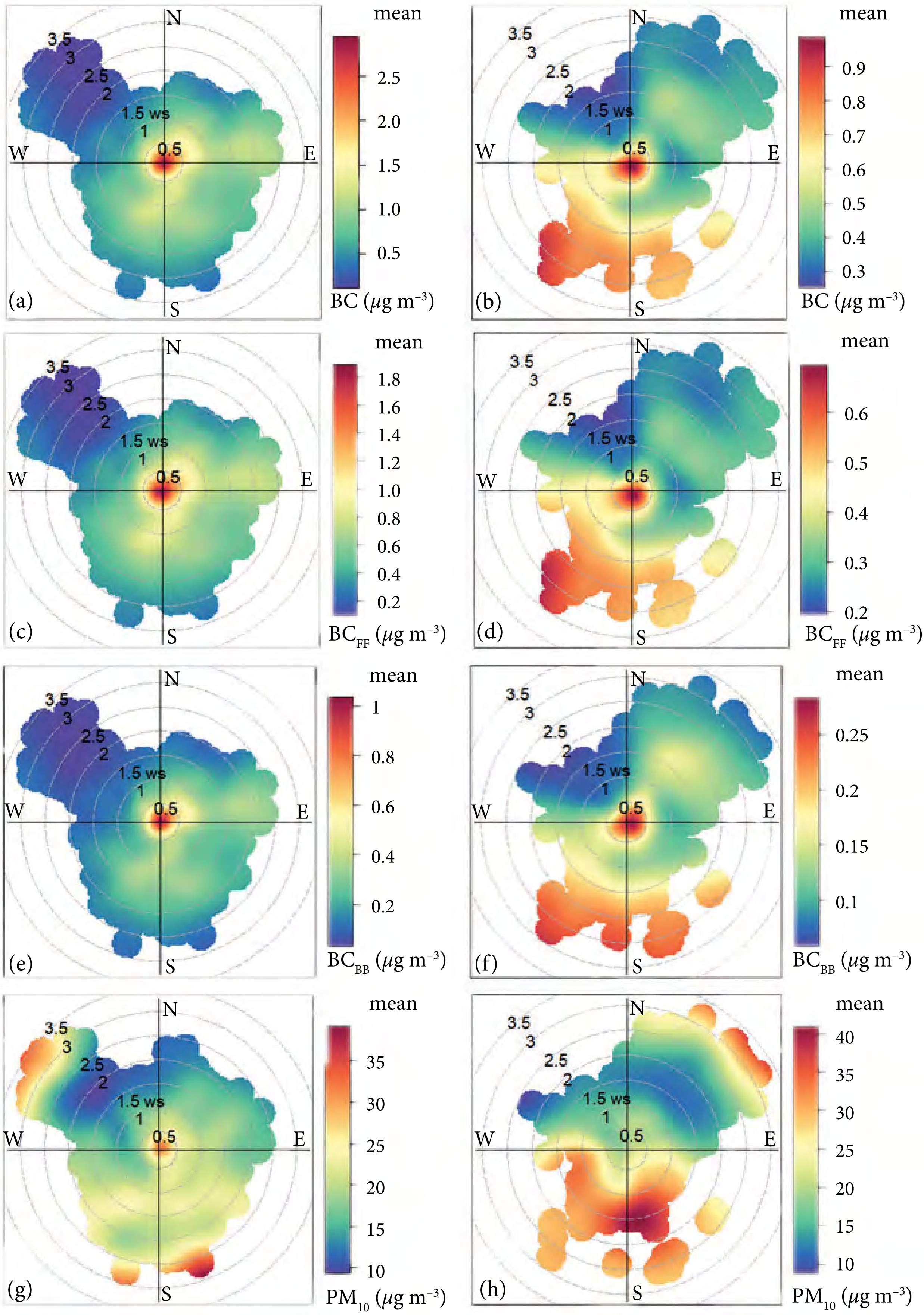

Fig. 7. Polar plots of BC, BC_{FF}, BC_{BB}, PM_{10} and NO_x mass concentration as a function of wind speed and direction for heating (a, c, e, g, i) and non-heating periods (b, d, f, h, j).

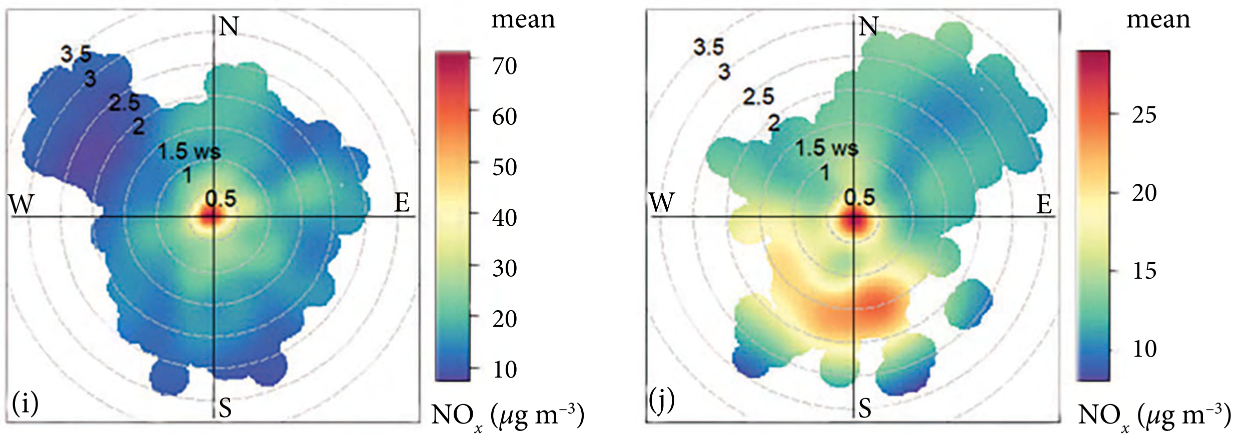

Fig. 7. (Continued) Polar plots of BC, BC_{FF}, BC_{BB}, PM_{10} and NO_x mass concentration as a function of wind speed and direction for heating (a, c, e, g, i) and non-heating periods (b, d, f, h, j).

4. Conclusions

With respect to seasonality, the BC mass concentrations are similar to those of other European cities and indicate the similar impact of traffic and heating – the major urban sources. The average BC mass concentration during the heating period (1.17 μg m^{-3}) was almost twice (1.92) higher than during the non-heating (0.61 μg m^{-3}) period in Vilnius. Fossil fuel combustion was a significant contributor to BC pollution throughout the year (71.1%), with a maximum (8.43 μg m^{-3}) during the heating period. During the heating period, the potential source area was predominantly evenly distributed around the sampling site for all wind directions for calm wind with speeds up to 0.5 m s^{-1}. While, in the non-heating period, it was primarily concentrated in the southwest region. Nevertheless, the mass concentration of PM_{10} remains relatively stable throughout both seasons (19.4 μg m^{-3} for the heating period and 20.0 μg m^{-3} for the non-heating one).

During both the heating and non-heating periods, a positive correlation (0.65 and 0.55, respectively) was observed between BC mass concentrations and NO_x. However, the relationship between BC and PM_{10} was weak (0.48), particularly in the non-heating period (0.26). Furthermore, the meteorological impact on BC, PM_{10} and NO_x concentrations was more pronounced during the heating period. The maximum negative correlation was observed between the wind speed and BC, NO_x (correlation coefficient of –0.40), while the maximum positive correlation was observed between the pressure and PM_{10} (correlation coefficient of 0.40). In contrast, the influence was relatively weak during the non-heating period, with the maximum (by absolute value) negative correlation of –0.21 observed between the wind speed and BC, NO_x, and the maximum positive correlation of 0.33 observed between the temperature and PM_{10}.

However, in the non-heating period season, there were some differences in the pattern. The concentrations of BC, BC_{FF}, BC_{BB} and NO_x were highest at varying wind speeds in the SE–S–SW directions. And for PM_{10}, the polar plot shows even stronger impacts from relatively distant sources in north-easterly directions at wind speeds above 3 m s^{-1}.

References

[1] O.A. Sindosi, N. Hatzianastassiou, G. Markozannes, E.C. Rizos, E. Ntzani, and A. Bartzokas, PM_{10} concentrations in a provincial city of inland Greece in the times of austerity and their relationship with meteorological and socioeconomic conditions, Water Air Soil Pollut. **232**, 77 (2021).

[2] N. Zioła, B. Błaszczak, and K. Klejnowski, Temporal variability of equivalent black carbon components in atmospheric air in Southern Poland, Atmosphere (Basel) **12**, 119 (2021).

[3] B. Alfoldy, M.M. Mahfouz, A. Gregorič, M. Ivančič, I. Ježek, and M. Rigler, Atmospheric concentrations and emission ratios of black carbon and nitrogen oxides in the Arabian/Persian gulf region, Atmos. Environ. **256**, 118451 (2021).

[4] X. Liu, Y. Wei, X. Liu, L. Zu, B. Wang, S. Wang, R. Zhang, and R. Zhu, Effects of winter heating on urban black carbon: Characteristics, sources and its correlation with meteorological factors, Atmosphere (Basel) **13**, 1071 (2022).

[5] European Environment Agency, *Air Quality in Europe 2021*, EEA Report No. 15/2021 (Publications Office of the European Union, 2021).

[6] K. Bodor, M.M. Micheu, Á. Keresztesi, M.V. Birsan, I.A. Nita, Z. Bodor, S. Petres, A. Korodi, and R. Szép, Effects of PM_{10} and weather on respiratory and cardiovascular diseases in the Ciuc Basin (Romanian Carpathians), Atmosphere **12**, 289 (2021).

[7] M. Renzi, F. Forastiere, J. Schwartz, M. Davoli, P. Michelozzi, and M. Stafoggia, Long-term PM_{10} exposure and cause-specific mortality in the Latium Region (Italy): A difference-in-differences approach, Environ. Health Perspect. **127**, 067004 (2019).

[8] C.B.B. Guerreiro, V. Foltescu, and F. de Leeuw, Air quality status and trends in Europe, Atmos. Environ. **98**, 376 (2014).

[9] X. Yangyang, Z. Bin, Z. Lin, and L. Rong, Spatiotemporal variations of $PM_{2.5}$ and PM_{10} concentrations between 31 Chinese cities and their relationships with SO_2, NO_2, CO and O_3, Particuology **20**, 141–149 (2015).

[10] S.K. Pani, S.H. Wang, N.H. Lin, S. Chantara, C. Te Lee, and D. Thepnuan, Black carbon over an urban amosphere in Northern Peninsular Southeast Asia: Characteristics, source apportionment, and associated health risks, Environ. Pollut. **259**, 113871 (2020).

[11] H. Zhou, J. Lin, Y. Shen, F. Deng, Y. Gao, Y. Liu, H. Dong, Y. Zhang, Q. Sun, J. Fang, et al., Personal black carbon exposure and its determinants among elderly adults in urban China, Environ. Int. **138**, 105607 (2020).

[12] I. Cunha-Lopes, V. Martins, T. Faria, C. Correia, and S.M. Almeida, Children's exposure to sized-fractioned particulate matter and black carbon in an urban environment, Build. Environ. **155**, 187 (2019).

[13] S.F. Suglia, A. Gryparis, R.O. Wright, J. Schwartz, and R.J. Wright, Association of black carbon with cognition among children in a prospective birth cohort study, Am. J. Epidemiol. **167**, 280 (2008).

[14] M.P. Raju, P.D. Safai, S.M. Sonbawne, P.S. Buchunde, G. Pandithurai, and K.K. Dani, Black carbon aerosols over a high altitude station, Mahabaleshwar: Radiative forcing and source apportionment, Atmos. Pollut. Res. **11**, 1408 (2020).

[15] M. Kucbel, A. Corsaro, B. Švédová, H. Raclavská, K. Raclavský, and D. Juchelková, Temporal and seasonal variations of black carbon in a highly polluted European city: Apportionment of potential sources and the effect of meteorological conditions, J. Environ. Manage. **203**, 1178 (2017).

[16] A. Farah, P. Villani, C. Rose, S. Conil, L. Langrene, P. Laj, and K. Sellegri, Characterization of aerosol physical and optical properties at the Observatoire Perenne de l'Environnement (OPE) Site, Atmosphere (Basel) **11**, 172 (2020).

[17] M. Viana, S. Díez, and C. Reche, Indoor and outdoor sources and infiltration processes of PM_1 and black carbon in an urban environment, Atmos. Environ. **45**, 6359 (2011).

[18] A. Helin, J.V. Niemi, A. Virkkula, L. Pirjola, K. Teinilä, J. Backman, M. Aurela, S. Saarikoski, T. Rönkkö, E. Asmi, and H. Timonen, Characteristics and source apportionment of black carbon in the Helsinki metropolitan area, Finland, Atmos. Environ. **190**, 87 (2018).

[19] E. Hristova, E. Georgieva, B. Veleva, N. Neykova, S. Naydenova, L. Gonsalvesh-Musakova, R. Neykova, and A. Petrov, Black carbon in Bulgaria – observed and modelled concentrations in two cities for two months, Atmosphere (Basel) **13**, 213 (2022).

[20] M. Piñeiro-Iglesias, J. Andrade-Garda, S. Suárez-Garaboa, S. Muniategui-Lorenzo, P. López-Mahía, and D. Prada-Rodríguez, Study of temporal variations of equivalent black carbon in a coastal city in northwest Spain using an atmospheric aerosol data management software, Appl. Sci. **11**, 1 (2021).

[21] S. Mbengue, N. Serfozo, J. Schwarz, N. Ziková, A.H. Šmejkalová, and I. Holoubek, Characterization of equivalent black carbon at a regional background site in Central Europe: Variability and source apportionment, Environ. Pollut. **260**, 113771 (2020).

[22] E. Diapouli, A.C. Kalogridis, C. Markantonaki, S. Vratolis, P. Fetfatzis, C. Colombi, and K. Eleftheriadis, Annual variability of black carbon concentrations originating from biomass and fossil fuel combustion for the suburban aerosol in Athens, Greece, Atmosphere (Basel) **8**, 234 (2017).

[23] J. Deng, H. Guo, H. Zhang, J. Zhu, X. Wang, and P. Fu, Source apportionment of black carbon aerosols from light absorption observation and source-oriented modeling: an implication in a coastal city in China, Atmos. Chem. Phys. **20**, 14419 (2020).

[24] S. Byčenkienė, V. Ulevičius, and S. Kecorius, Characteristics of black carbon aerosol mass concentration over the East Baltic Region from two-year measurements, J. Environ. Monit. **13**, 1027 (2011).

[25] S. Byčenkienė, V. Dudoitis, and V. Ulevičius, The use of trajectory cluster analysis to evaluate the long-range transport of black carbon aerosol in the South-Eastern Baltic Region, Adv. Meteorol. **2014**, 11 (2014).

[26] J. Pauraitė, G. Mordas, S. Byčenkienė, and V. Ulevičius, Spatial and temporal analysis of organic and black carbon mass concentrations in Lithuania, Atmosphere (Basel) **6**, 1229 (2015).

[27] V. Ulevičius, S. Byčenkienė, V. Remeikis, A. Garbaras, S. Kecorius, J. Andriejauskienė, D. Jasinevičienė, and G. Mocnik, Characterization of pollution events in the East Baltic region affected by regional biomass fire emissions, Atmos. Res. **98**, 190 (2010).

[28] K. Kvietkus, J. Šakalys, J. Didžbalis, I. Garbarienė, N. Špirkauskaitė, and V. Remeikis, Atmospheric aerosol episodes over Lithuania after the May 2011 volcano eruption at Grimsvötn, Iceland, Atmos. Res. **122**, 93 (2013).

[29] A. Minderytė, E.A. Ugboma, F.F. Mirza Montoro, I.S. Stachlewska, and S. Byčenkienė, Impact of long-range transport on black carbon source contribution and optical aerosol properties in two urban environments, Heliyon **9**, 19652 (2023).

[30] S. Saarikoski, J.V. Niemi, M. Aurela, L. Pirjola, A. Kousa, T. Rönkkö, and H. Timonen, Sources of black carbon at residential and traffic environments obtained by two source apportionment methods, Atmos. Chem. Phys. **21**, 14851–14869 (2021).

[31] E. Ezani, S. Dhandapani, M.R. Heal, S.M. Praveena, M.F. Khan, and Z.T.A. Ramly, Characteristics and source apportionment of black carbon (Bc) in a suburban area of Klang valley, Malaysia, Atmosphere (Basel) **12**, 1 (2021).

[32] J. Sandradewi, A.S.H. Prévôt, S. Szidat, N. Perron, M.R. Alfarra, V.A. Lanz, E. Weingartner, and U. Baltensperger, Using aerosol light absorption measurements for the quantitative determination of wood burning and traffic emission contributions to particulate matter, Environ. Sci. Technol. **42**, 3316 (2008).

[33] C. Mandin, M. Trantallidi, A. Cattaneo, N. Canha, V.G. Mihucz, T. Szigeti, R. Mabilia, E. Perreca, A. Spinazzè, S. Fossati, et al., Assessment of indoor air quality in office buildings across Europe – The OFFICAIR Study, Sci. Total Environ. **579**, 169 (2017).

[34] World Health Organization, *Review of Evidence on Health Aspects of Air Pollution – REVIHAAP Project*, Technical Report (World Health Organization Regional Office for Europe, 2013).

[35] A. Minderytė, J. Pauraitė, V. Dudoitis, K. Plauškaitė, A. Kilikevičius, J. Matijošius, A. Rimkus, K. Kilikevičienė, D. Vainorius, and S. Byčenkienė, Carbonaceous aerosol source apportionment and assessment of transport-related pollution, Atmos. Environ. **279**, 119043 (2022).

[36] M. Becerril-Valle, E. Coz, A.S.H. Prévôt, G. Močnik, S.N. Pandis, A.M. Sánchez de la Campa, A. Alastuey, E. Díaz, R.M. Pérez, and B. Artíñano, Characterization of atmospheric black carbon and co-pollutants in urban and rural areas of Spain, Atmos. Environ. **169**, 36 (2017).

[37] X. Liu, H. Hadiatullah, P. Tai, Y. Xu, X. Zhang, J. Schnelle-Kreis, B. Schloter-Hai, and R. Zimmermann, Air pollution in Germany: Spatio-

temporal variations and their driving factors based on continuous data from 2008 to 2018, Environ. Pollut. **276**, 116732 (2021).

[38] M.S. Al Rashidi, Assessment of the atmospheric mixing layer height and its effects on pollutant dispersion, Environ Monit Assess. **190**, 371 (2018).

JUODOSIOS ANGLIES, KIETŲJŲ DALELIŲ IR AZOTO OKSIDŲ MASĖS KONCENTRACIJŲ KITIMAS MIESTO APLINKOJE, ATSIŽVELGIANT Į ŽIEMOS ŠILDYMO LAIKOTARPĮ IR METEOROLOGINES SĄLYGAS

D. Pashneva, A. Minderytė, L. Davulienė, V. Dudoitis, S. Byčenkienė

Valstybinis mokslinių tyrimų institutas Fizinių ir technologijos mokslų centras, Vilnius, Lietuva

Santrauka

Atmosferos tarša aerozolio arba kietosiomis dalelėmis (KD) kelia didelį mokslininkų susirūpinimą dėl jų poveikio žmonių sveikatai ir aplinkos taršai. Šio tyrimo tikslas – ištirti juodosios anglies (BC), kietųjų dalelių, kurių aerodinaminis skersmuo ne didesnis kaip 10 mikrometrų (KD_{10}), ir azoto oksidų (NO_x) koncentraciją miesto foninėje aplinkoje ištisus metus ir išsiaiškinti žiemos šildymo bei meteorologinių sąlygų įtaką jų koncentracijos lygiui. Matavimai vyko šildymo ir nešildymo sezonų metu nuo 2021 m. birželio 1 d. iki 2022 m. gegužės 31 d. Šildymo laikotarpiu BC, KD_{10} ir NO_x masės koncentracijos ore siekė 1,17, 24,9 ir 19,4 μg m^{-3}, atitinkamai. Analizė parodė, kad BC ir NO_x masės koncentracijos lygiai šildymo laikotarpiu buvo 1,9 ir 1,4 karto, atitinkamai, didesnės palyginti su šiltuoju laikotarpiu. Priešingai, KD_{10} koncentracijos lygis šaltuoju sezonu (19,4 μg m^{-3}) išliko panašus palyginti su šiltuoju laikotarpiu (20,0 μg m^{-3}). Nustatyta, kad tyrimo metu vyravo iškastinio kuro deginimo kilmės juodosios anglies BC_{FF} koncentracijos indėlis (71,2 %) į bendrą masės koncentraciją, kurios didžiausia stebėta vertė šildymo laikotarpiu siekė 8,43 μg m^{-3}. Be to, pastebėta, kad šildymo laikotarpiu vėjo greitis turėjo silpną neigiamą koreliaciją su BC ($r = -0{,}40$), KD_{10} ($r = -0{,}19$) ir NO_x ($r = -0{,}40$).